

NASA Technical Memorandum 102371

Characterization of Failure Processes in Tungsten Copper Composites Under Fatigue Loading Conditions

K

Yong-Suk Kim, Michael J. Verrilli, and Timothy P. Gabb
Lewis Research Center
Cleveland, Ohio

Prepared for the
International Symposium for Testing and Failure Analysis (ISTFA '89)
sponsored by ASM International
Los Angeles, California, November 6-10, 1989

NASA

(NASA-TM-102371) CHARACTERIZATION OF
FAILURE PROCESSES IN TUNGSTEN COPPER
COMPOSITES UNDER FATIGUE LOADING CONDITIONS
(NASA) 102371

CSCL 310

N70-01110

unc135

05/24 0272540

Trade names or manufacturers' names are used in this report for identification only. This usage does not constitute an official endorsement, either expressed or implied, by the National Aeronautics and Space Administration.

CHARACTERIZATION OF FAILURE PROCESSES IN TUNGSTEN COPPER COMPOSITES UNDER FATIGUE LOADING CONDITIONS

Yong-Suk Kim*, Michael J. Verrilli, and Timothy P. Gabb
National Aeronautics and Space Administration
Lewis Research Center
Cleveland, Ohio 44135

SUMMARY

A fractographic and metallographic investigation was performed on specimens of a tungsten-fiber-reinforced copper matrix composite (9 vol %), which had experienced fatigue failures at elevated temperatures. The aim of the study was to determine major failure modes and possible failure mechanisms, with an emphasis placed on characterizing fatigue damage accumulation. Metallography of specimens fatigued under isothermal cyclic loading suggested that fatigue damage initiates in the matrix. Cracks nucleated within the copper matrix at grain boundaries, and they propagated through cavity coalescence. The growing cracks subsequently interacted with the reinforcing tungsten fibers, producing a localized ductile fiber failure. Examinations of interrupted tests before final failure confirmed the suggested fatigue damage processes.

INTRODUCTION

Many high-temperature engineering applications require the use of materials with specialized properties such as increased toughness, stiffness, strength, fatigue resistance, and use temperature. Continuous-fiber-reinforced metal matrix composites are among these advanced high-temperature materials because they can be used under high-temperature conditions without significant loss of stiffness. Since metal matrix composite materials are targeted for uses in critical engineering components, prediction of durability is a crucial requirement. An understanding of the dominant failure mechanism is indispensable for the proper prediction of lifetime. However, the failure mechanisms of composite materials are not sufficiently understood yet, especially under cyclic-loading conditions at high temperatures.

Currently a Cu alloy is used as a combustion chamber liner material for the space shuttle main engine. The large temperature gradient within the liner during a rocket launch causes large, thermally induced, cyclic plastic deformation of the liner material. For improved durability in this application, NASA Lewis Research Center personnel are considering a tungsten-fiber-reinforced copper composite (W/Cu) as a substitute material. Therefore the high-temperature fatigue properties of this material are being characterized.

Fiber-reinforced composite materials can be generally categorized into three types: (1) brittle fibers in a brittle matrix, (2) brittle fibers in a ductile matrix, and (3) ductile fibers in a ductile matrix. The operative

*National Research Council - NASA Research Associate.

failure mechanisms of composites generally vary from category to category. The tungsten-fiber-reinforced copper composite is a ductile-ductile type material. Many researchers have used this system as a model composite material because of the strong and stable interface between its composite constituents and the relative ease with which it is manufactured (refs. 1 to 10). However, most past work on this composite system has dealt with room temperature deformation behavior (refs. 3 to 6), elevated temperature tensile response (ref. 7), and simple thermal cycling effects (refs. 1,2,8, and 9). Cyclic test results of the composite at high temperatures are rare, and failure mechanisms under such loading conditions have seldom been reported (ref. 10).

This paper presents preliminary results of ongoing research on the W/Cu composite and focuses on evaluating the failure mechanisms of the composite in isothermal fatigue at temperatures of 533 and 833 K. The results obtained through fractographic analyses with SEM and optical microscopy are reported along with a characterization of outside surface damage. Detailed mechanical results of fatigue tests of the composite are reported in another paper (ref. 11).

EXPERIMENTAL PROCEDURES

Material and Specimen

The W/Cu composite used in this study was manufactured by Westinghouse Electric Corporation (Pittsburgh, PA) through an arc-spraying technique (ref. 12). The matrix material was an oxygen-free, high-conductivity (OFHC) copper (99.95 wt % Cu) with 200- μ m-diameter G.E. 218 tungsten wires used as the reinforcing fiber. The as-received composite was a thin plate (2.54 mm thick) composed of four plies of W/Cu monotapes. The fiber volume fraction measured in all test specimens was 9 ± 0.5 vol %. Rectangular cross-section specimens (fig. 1) were machined directly from the as-received composite plate by using electrodischarge machining. Specimens tested in the present work have only one orientation: all fibers are aligned parallel to the loading direction.

MECHANICAL TESTING

Fatigue tests were carried out with a closed-loop-servo-hydraulic machine at 533 and 833 K in a vacuum of 10^{-6} torr. The cyclic loading used a triangular wave form at a frequency of 3 cpm. All tests were performed in a load control mode with an approximate R ratio (minimum load/maximum load) of 0.05. Most of the specimens were cycled to complete failure, but some were interrupted before failure in order to examine the evolution of the fatigue damage. Further information on the fatigue tests is provided in another paper (ref. 11).

In order to differentiate between creep and fatigue processes in the failure of the composite, several monotonic creep tests were also performed. Constant-load, creep-rupture tests were performed in vacuum at 533 K. After creep rupture, the fracture surfaces and cross sections were examined in a manner similar to the fatigue-fractured specimens.

Microhardness indentations were made with a 25-g load on sections cut through tested specimens. Vickers hardness was measured in the matrix to give quantitative indications of the amount of strain hardening in tested specimens and the possible residual stresses due to the manufacturing processes of the composite.

FAILURE ANALYSIS

Fractographic and metallographic studies were employed to evaluate the failure mechanism of the composite. A scanning electron microscope operating with an accelerating voltage of 25 kV was employed for the fractographic study. Extensive metallography was performed to examine the sectioned surfaces of failed specimens.

EXPERIMENTAL RESULTS

Microstructure

The microstructure of the as-received composite was examined with an optical microscope (fig. 2). Figure 2 shows both the Cu matrix and the periodically arranged W fibers. The interspacing between fibers is not regular, and the matrix grain size varies with locations. Figure 3 is an enlarged micrograph of the as-received composite. The uneven grain size distribution in the Cu matrix is well displayed. The grain sizes are in the range of 8 to 15 μm . Usually, finer grains are observed near the fiber, whereas large grains occur between fibers. No interface reaction products were observed, which is consistent with other studies (refs. 1 to 10).

FATIGUE TEST RESULTS

Figure 4 shows some of the fatigue test results as a linear-log plot of the maximum cyclic strain per cycle versus the applied number of cycles. Test results from both 533 and 833 K are plotted together. At both temperatures the maximum strain in each cycle increases (ratchets) continuously until the specimen fails. This behavior is analogous to typical secondary and tertiary strain versus time behavior in the creep of a monolithic material. For comparison, the results of a creep test for the composite at 533 K is also shown in figure 4, as a linear-linear plot of strain versus time. This similarity in behavior will be shown to extend to the matrix failure mechanism as well. The total failure strain increases with increasing maximum cyclic stress at both temperatures. The total failure strain of the specimens tested at 533 K is larger than that tested at 833 K. Additional mechanical test results are reported elsewhere (ref. 11).

SURFACE DAMAGE EXAMINATION

The fatigue specimens tested to failure at 533 K show many small secondary edge cracks along the specimen edge, far from the dominant crack which led to failure. Figure 5 is a low-magnification micrograph of the side of a fractured specimen at 533 K. The fracture surface is indicated in the figure. As figure 5 shows, these side cracks were spaced at fairly regular intervals. Most

of the side cracks only extended to the first row of fibers and then stopped growing. In contrast, the specimens tested at 833 K did not develop as many secondary-edge cracks nor did they exhibit as much accumulated plastic strain.

In addition to the secondary-edge cracks, numerous other small secondary cracks were observed near the fracture surface along the broad sides of the specimen (fig. 6). These secondary cracks were again found mostly in specimens tested at 533 K and were not prevalent on specimens tested at 833 K. Some of these small secondary cracks were connected to the dominant crack and some were not. Unlike the secondary-edge cracks, the location of these smaller secondary cracks was confined near the fracture surface. The specimens tested at 833 K did not show significant secondary cracks. Instead, one single major crack was found to propagate as shown in figure 7.

FRACTOGRAPHIC STUDY

The observed fracture surface shows that the dominant crack propagated roughly transverse to the applied load, though microscopic observation reveals an irregular fatigue fracture morphology. It is very difficult to find a path of crack propagation (e.g., river patterns) on the fracture surface. Fiber pullouts are rarely observed in the specimens tested at either temperature. Rather, the Cu matrix often adhered to the failed tungsten fibers.

Figure 8 shows the fracture surface of a fatigue specimen tested at 533 K. The composite experienced ductile failure in both constituents. The fiber failure indicates large inelastic deformation that produced necking. The matrix failed in fatigue by a predominantly intergranular mode, whereas final tensile overload failure occurred by a predominantly transgranular mode.

Figure 9 is a magnified view of the failed matrix tested at 533 K. Figure 9(a) is a fractograph of an intergranular fatigue failure region, and figure 9(b) is a fractograph of a transgranular tensile failure region. Figure 9(a) clearly shows the intergranular failure mode, along with a very irregular grain size. No fatigue striation marks are observed, but the cracks and cavities along the grain boundaries are revealed. Figure 9(b) reveals a typical ductile overload failure region. In these specimens, the intergranularly fractured regions are mostly confined to the outer surface of the specimen and to the matrix surrounding the fiber. The ductile overload fracture normally occurs in the middle of the specimen, in the midregion between fibers.

The fractography of specimens tested at 833 K is different from that at 533 K. Most of the fracture surface exhibits an intergranular failure mode as shown in figure 10. Not much ductile overload failure is observed, even in the middle of the specimen. The magnified view of the intergranularly fractured surface shows more clearly formed grain boundary cavities than those for the 533 K tests.

To compare the fractography under different test conditions, we also examined the fracture surface of a creep specimen ruptured under a static load of 240 MPa at 533 K (fig. 11). Compared with the fatigue specimen tested at the same temperature, the matrix of the creep-ruptured specimen shows more predominant intergranular failure throughout the specimen cross section. However the fracture nature of the tungsten fiber varies little from the fatigue specimen: the fiber exhibits large plastic deformation.

The SEM observation of fractured surfaces also permitted the measurement of the reduction of area of tungsten fibers following cyclic failures. The reduction of area of 30 to 40 fibers was measured on each fracture surface. The measured reduction of area of the fibers was approximately 70 percent for all of the tests performed at the two elevated temperatures. The room temperature ductility of the fiber, however, is nil. The high reduction of area at these relatively low elevated temperatures (0.14 to 0.27 T_m) seems to be an inherent nature of the tungsten fiber, G.E. 218.

METALLOGRAPHIC STUDY

Figure 12 is an optical micrograph of a longitudinal section near the fracture surface of a specimen fatigue fractured at 533 K. The section shows one layer of fibers among the four plies which comprise the composite. Even though this section is not of the dominant crack, the secondary cracks shown in figure 12 can be assumed to be similar to those that occurred along the dominant fracture plane. The figure shows matrix cracks that are perpendicular to the loading direction and shows the fractured fibers. The cracks shown in figure 12 may have been widened during final failure of the specimen. However they still do provide information for crack initiation and propagation processes. The large crack opening displacement at the left side of the specimen indicates that the dominant crack initiated at the side of the specimen and propagated into the inner portion of the specimen.

Besides surface cracks, some cracks were observed to originate internally in the Cu matrix. The crack marked "B" in the figure is one of such cracks. The crack is independent from the propagating approaching crack, marked "A", and apparently it initiated separately. Subsequent examinations of underlying layers confirmed that these cracks were not connected.

The fibers are broken, forming nicely shaped necks at widely opened Cu matrix cracks, and fiber failure is not limited to the crack front. The fibers seem to break after the surrounding matrix degrades. The deformation of the fiber appears to be very localized, since the necking is confined within a very narrow region between the mating surfaces of the propagating crack.

MICROHARDNESS TEST

In order to assess the amount of strain hardening and residual stresses in the Cu matrix, a microhardness test has been utilized. Several indentations were made in the Cu matrix at equal intervals between fibers. A summary of quantitative microhardness measurements on the matrix material is shown in table I. The hardness numbers in table I are averages of a minimum of seven readings. The average value was used since no significant variation of microhardness values (independent of location) could be detected within the matrix. The scatter of each of the hardness values in table I was approximately ± 10 Hv.

As the values indicate, the difference in hardness readings of the specimens tested under different conditions was also negligible. These small differences suggest that the strain hardening in the Cu matrix due to fatigue testing and possible residual stresses was not great enough to be detected through this technique. These findings are consistent with Jones' work

(ref. 13). The softening of the matrix due to high-temperature annealing during fatigue tests was neglected for the present study, since vacuum annealing of the composite at the test temperatures without applied load did not show any significant softening of the Cu matrix.

DISCUSSION

The fatigued specimens at 533 and 833 K have shown significant differences. The Cu matrix of specimens tested at 533 K had more secondary cracks, and the damage formation inside the Cu matrix (including cracks and cavities) at this temperature seemed to be a global phenomenon, not a localized one. The 833 K specimens showed few secondary cracks in the Cu matrix. These differences at the two test temperatures seem to be associated with the difference in the failure strain (ductility) which the composite experienced during the cyclic loading. As noted in the former section, the specimens tested at 833 K had a smaller cyclic failure strain. The decrease of the composite's failure strain with increasing temperature is believed to be due to the failure mode change of the Cu matrix.

It has been reported that Cu loses its ductility as temperature increases because of an enhancement of cavitation along grain boundaries (ref. 14). The effect of the W fiber on the composite failure behavior with temperature changes seems to be small. The fatigue behavior of the W fibers at the two temperatures were similar. Bartolotta et al. (P.A. Bartolotta, P.K. Brindley, and J.R. Ellis, 1989, NASA TM, to be published.) investigated the relationship between the fiber failure mode and the total failure strain of a tungsten-fiber-reinforced superalloy composite (35 vol %), which is also a ductile-ductile system. They reported that the total failure strain does not change significantly with fiber failure characteristics whether the fiber failure is brittle or ductile. The observations from these two references indicate the importance of the matrix deformation in the composite failure during cyclic loading.

Figure 13 is an SEM micrograph of the Cu matrix near the fracture surface. The grain boundaries are severely damaged. Many cavities are revealed, and some of them are linked to form short cracks. This figure indicates that the intergranular failure was caused by cavity nucleation and coalescence processes along grain boundaries. The metallographic observations combined with the fractographs reveal that under the given test conditions cracks mostly initiate inside the Cu matrix at the outer surface of a specimen. They then propagate towards the center of the specimen intergranularly by cavity growth and coalescence processes.

The fiber-matrix interface was carefully examined and no cracks or debonding were observed. Compared with other metal matrix composites, the W/Cu system exhibits no interfacial reaction products (refs. 1 to 10) although the exact bond type is unknown. The specimens tested at 533 and 833 K also show that the interface remained stable during testing, and no degradation phenomena or reaction products have been observed. Figure 14 shows a deformed fiber with a neck. The Cu matrix still adheres to the deforming fiber, and the adjacent matrix, - not the interface - is being cracked. In thermo-mechanical fatigue tests, the interface may be a weak, crack-initiation location. The interface may degrade under such conditions. Yoda et al. (ref. 8) found that

pores form at the fiber/matrix interface during simple thermal cycling with the same material. The failure mechanisms of the composite under such test conditions are currently being investigated.

The fatigue failure of the composite strongly depends on the grain size of the matrix. Figure 15 shows how the grain size affects the failure of the composite. The small-grain region has more cavities than the large-grain region, and cracks propagate more readily through the small-grain region. Currently, the authors believe that the grain size effect is related to grain boundary sliding (GBS). Together with slip and diffusion, GBS is a well-known deformation process in fine-grain materials. Luthy et al. (ref. 15) modified the Ashby Deformation Map by including GBS as another deformation mechanism. They showed that GBS plays an important role at all temperatures in the deformation of a fine-grain material. Even though the composite specimen experienced only tension-tension cyclic loading, the Cu matrix is believed to experience compressive stresses during the unloading cycle because of the repeated plasticity and cyclic relaxation of the tensile matrix stresses. Repeated tension and compression inside the Cu matrix results in cyclic shear stresses that promote grain boundary sliding. It has also been reported that a wedge-type cavitation prevails when grain boundary sliding is a major deformation mode (ref. 16). Some SEM pictures and optical micrographs from an early stage of cavitation in an interrupted test specimen show more wedge-type cavitation than r-type cavitation. This observation again supports the view that the composite matrix experiences grain boundary sliding under the given loading conditions and temperatures. A specimen with a large-grain matrix could have a prolonged life under the same loading conditions because of the decreased chance of grain boundary sliding. Testing and analyses to further confirm these findings are currently underway.

Another interesting observation related to the cavity nucleation and growth is that, in many regions of the Cu matrix, very irregular cavity distributions are found. Figure 16 shows a typical example of this irregular cavity distribution. The composite has fewer cavities near the fiber/matrix interface, and the cavities are frequently observed to be aligned with some degree of regularity. Most of the time, the cavities are spread parallel to the loading or fiber direction. This uneven distribution of cavities is believed to be related to the stress redistribution created by the fibers and the actual mechanical loading.

The failure of the composite under the given test conditions can be summarized as follows. Initially cracks were formed through plastic deformation in the Cu matrix mostly at outer surfaces. Multiple cracks were initiated depending on the amount of plastic deformation that the matrix experienced. After a major crack was formed, the crack propagated by cavity growth and coalescence processes. The breakage of fibers always came after the degradation of the surrounding matrix. The fibers were not cracked when the approaching cracks reached the fiber. After the crack propagated past the fiber and the surrounding matrix separated, the fiber deformed (with necking) and failed locally in a ductile failure mode. The final failure of the composite occurred when a sufficient area of a cross section of the specimen was cracked.

SUMMARY AND CONCLUSIONS

The failure mechanisms of a W-fiber-reinforced Cu matrix composite (9 vol %) were studied by using fractographic and metallographic techniques after isothermal cyclic loading at 533 and 833 K. The following is a summary of the findings:

1. The deformation of the Cu matrix strongly controls the failure of the W/Cu composite under the given test conditions.
2. Cracks are initiated inside the Cu matrix and propagate through cavity nucleation and coalescence processes.
3. The crack initiation and propagation resistance strongly depend on matrix grain size. Finer grain size accelerated crack initiation and propagation. More study of cavity growth under fatigue loading conditions at high temperatures is required for a detailed failure mechanism evaluation.
4. The fibers break after the surrounding matrix fails. The fibers fail locally by necking with a ductile failure mode.
5. Little strain hardening and residual stresses have been observed in the tested specimens by using the microhardness measurement technique.

REFERENCES

1. K.K. Chawla: Metallography, 1973, vol. 6, pp. 155-169.
2. K.K. Chawla: Philos. Mag., 1973, vol. 28, pp. 401-413.
3. A. Kelly, and W. R. Tyson: J. Mech. Phys. Solids, 1965, vol. 13, pp. 329-350.
4. R.E. Lee, and S.J. Harris: J. Mat. Sci., 1974, vol. 9, pp. 359-368.
5. K. Wakashima, T. Kawakubo, and S. Umekawa: Metall Trans. A, 1975, vol. 6A, pp. 1755-1760.
6. D.L. McDanel, R.W. Jech, and J.W. Weeton, AIME Trans., 1965, vol. 233, pp. 636-642.
7. D.W. Petrasek, AIME Trans., 1966, vol. 236, pp. 887-896.
8. S.R. Yoda, Takahashi, K. Wakashima, and S. Umekawa: Metall. Trans. A, 1979, vol. 10A, pp. 1796-1798.
9. S. Yoda, S., N. Kurihara, K. Wakashima, and S. Umekawa, Metall. Trans. A, 1978, vol. 9A, pp. 1229-1236.
10. D.L. McDanel: Tungsten Fiber Reinforced Copper Composites. NASA TP-2924, 1989.

11. Verrilli, M., Yong-Suk Kim, and T.P. Gabb: High Temperature Fatigue Behavior of Tungsten Copper Composite. Symposium on Fundamental Relationships Between Microstructure and Mechanical Properties of Metal-Matrix Composites, Indiana, October 1-5, 1989.
12. L.J. Westfall: Tungsten Fiber Reinforced Superalloy Composite Monolayer Fabrication by an ARC SPRAY Process. NASA TM-86917 (1985).
13. R.C. Jones: Metal Matrix Composites, pp. 183-217, ASTM STP-438, ASTM, Philadelphia, PA, 1968.
14. Nieh, T.G. and W.D. Nix: Metall Trans. A, 1981, vol. 12A, 893-901.
15. H. Luthy, R.A. White, and O.D. Sherby: Mater Sci. Eng., 1979, vol. 39, pp. 211-216.
16. Baik, S., and R. Raj, Metall Trans. A, 1982, vol. 13A, pp. 1207-1214.

TABLE I. - MICROHARDNESS TEST RESULTS
OF THE CU MATRIX

Test condition	Average Vickers hardness, Hv
As received	78
Tensile fracture at 533 K	80
Fatigue fracture at 533 K	87
Tensile fracture at 833 K	81
Fatigue fracture at 833 K	86

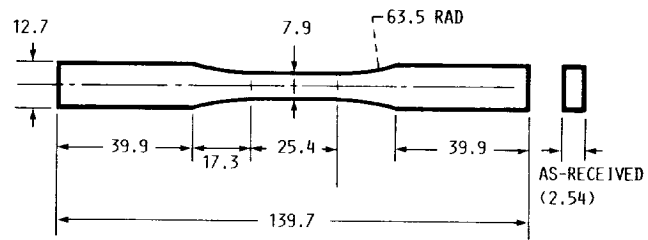


FIGURE 1. - SCHEMATIC DIAGRAM OF A RECTANGULAR SPECIMEN. ALL DIMENSIONS ARE GIVEN IN MILLIMETERS UNLESS MARKED OTHERWISE.

ORIGINAL PAGE
BLACK AND WHITE PHOTOGRAPH

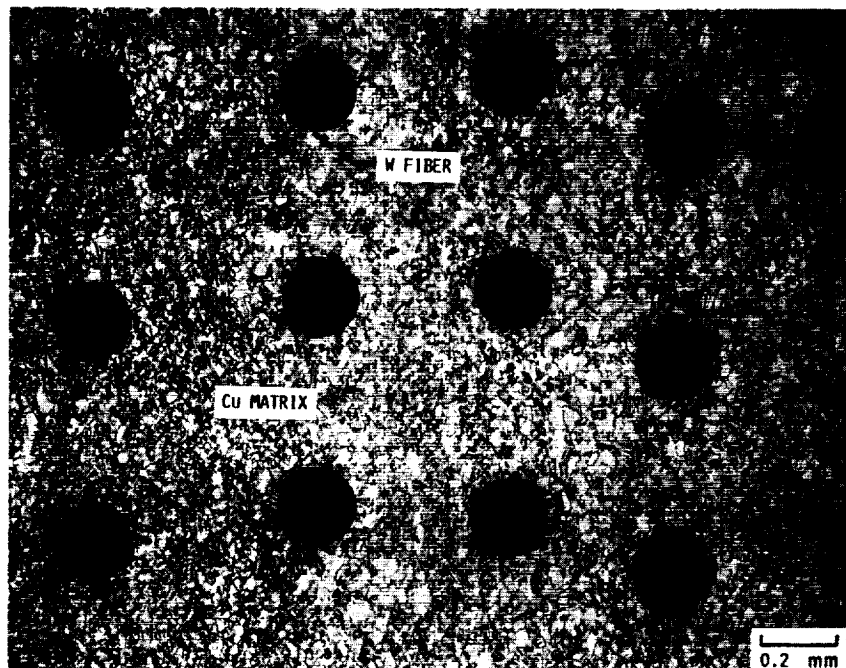


FIGURE 2. - AS-RECEIVED COMPOSITE SHOWING PERIODICALLY ARRANGED W FIBERS IN THE Cu MATRIX.

ORIGINAL PAGE
BLACK AND WHITE PHOTOGRAPH

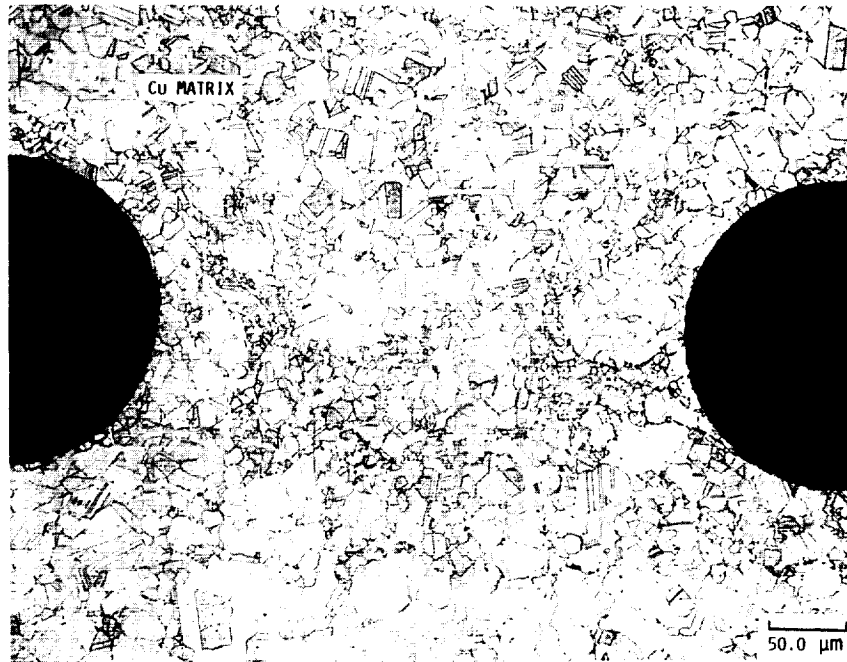


FIGURE 3. - MAGNIFIED MICROGRAPH OF AN AS RECEIVED W/Cu COMPOSITE. NOTE THE UNEVEN DISTRIBUTION OF GRAIN SIZES IN THE Cu MATRIX.

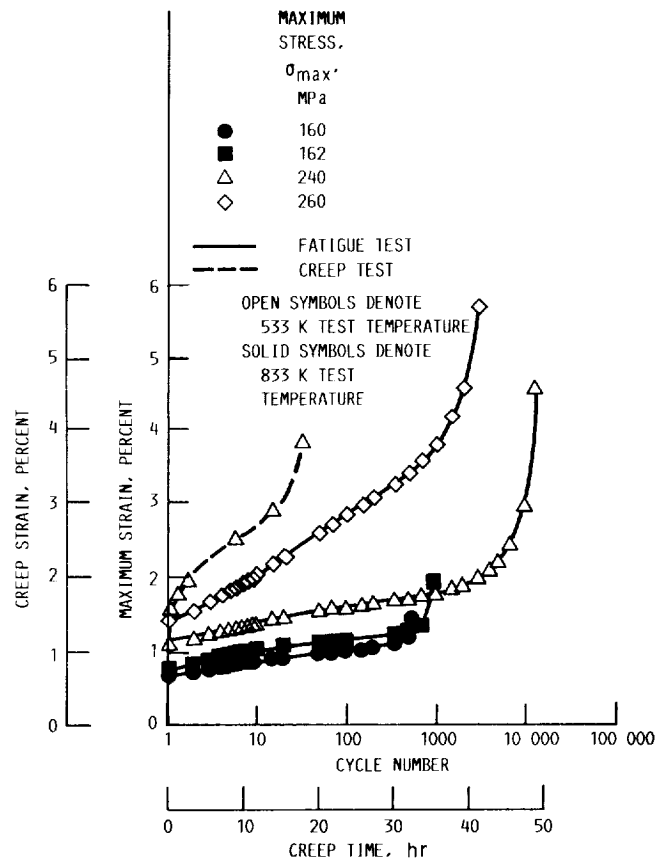


FIGURE 4. - MAXIMUM CYCLE STRAIN VERSUS NUMBER OF CYCLES FOR 9 vol % W-REINFORCED Cu TESTED UNDER LOAD-CONTROLLED FATIGUE AT 533 AND 833 K. FOR COMPARISON, A CREEP CURVE OF THE COMPOSITE AT 533 K AND AT 240 MPa IS ALSO SHOWN.

ORIGINAL PAGE IS
OF POOR QUALITY

ORIGINAL PAGE
BLACK AND WHITE PHOTOGRAPH

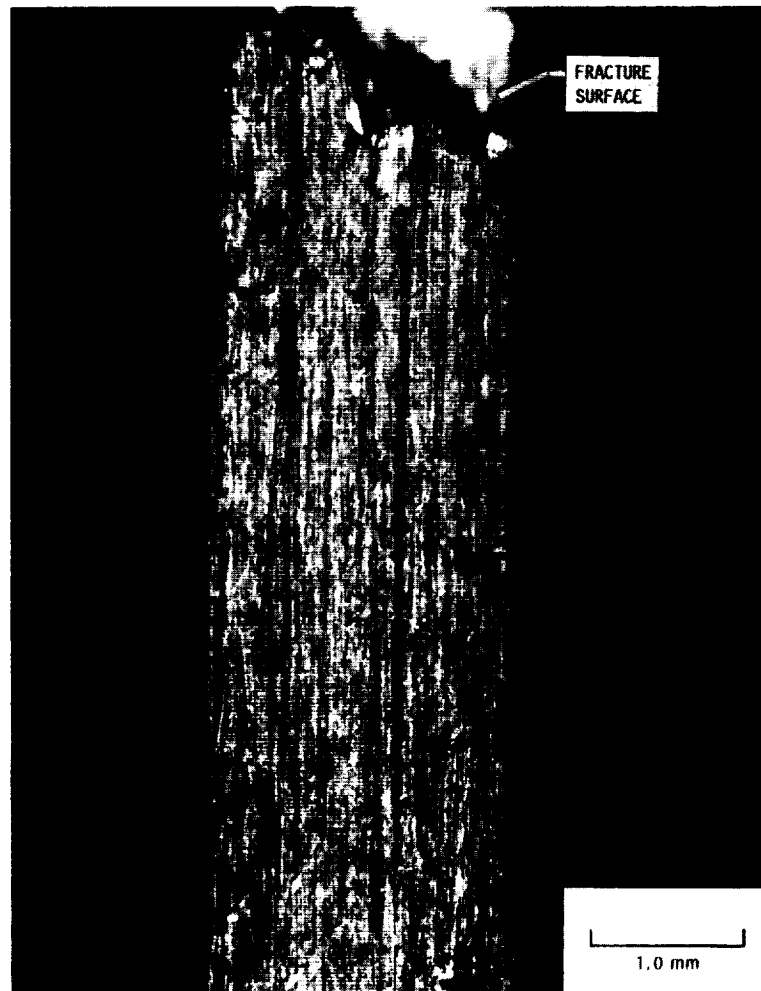


FIGURE 5. - A SIDE VIEW OF A FATIGUE SPECIMEN FRACTURED AT 533 K. THE MAXIMUM APPLIED STRESS IS 280 MPa, AND THE SPECIMEN FAILED AFTER 933 CYCLES.

ORIGINAL PAGE
OF POOR QUALITY

ORIGINAL PAGE
BLACK AND WHITE PHOTOGRAPH

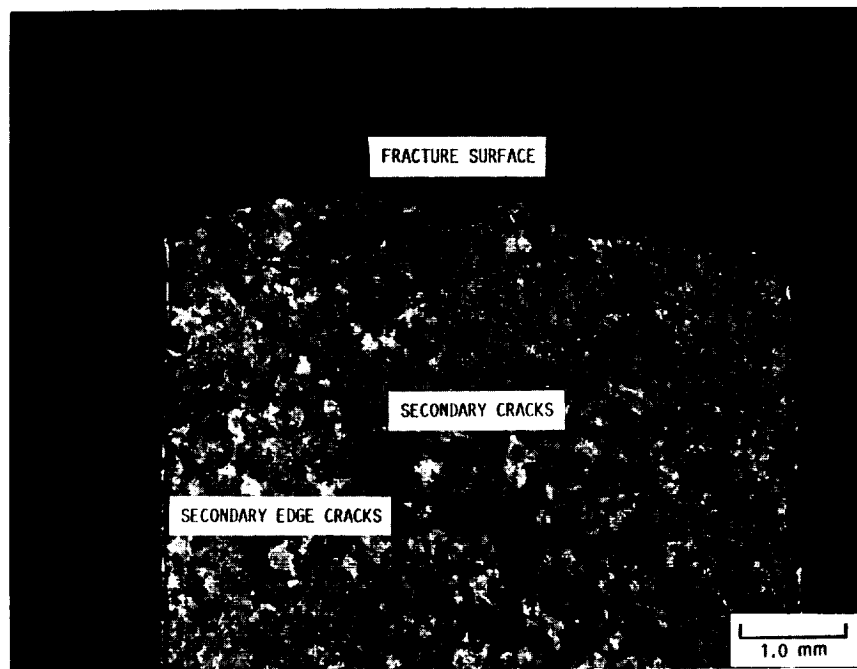


FIGURE 6. - BROADSIDE VIEW OF A FATIGUE SPECIMEN FRACTURED AT 533 K SHOWING NUMEROUS SECONDARY CRACKS.

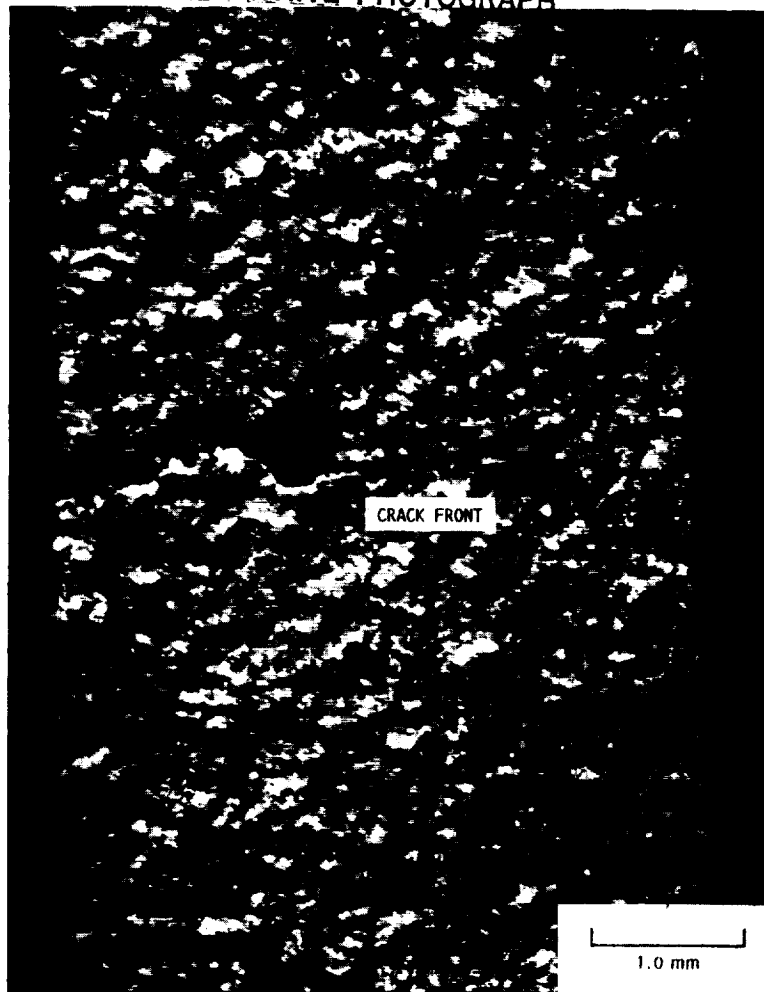


FIGURE 7. - SURFACE OF A SPECIMEN FATIGUED AT 833 K WITH A MAXIMUM STRESS OF 150 MPa. A DOMINANT CRACK IS OBSERVED WITH FEW SECONDARY CRACKS.

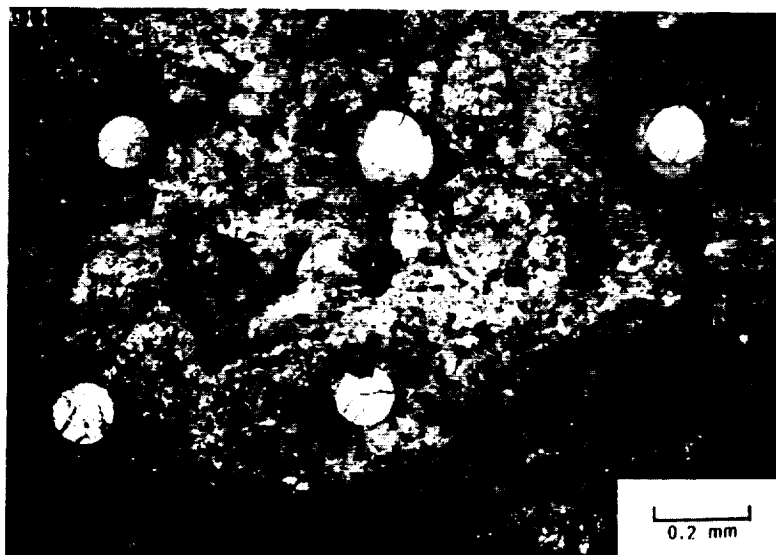
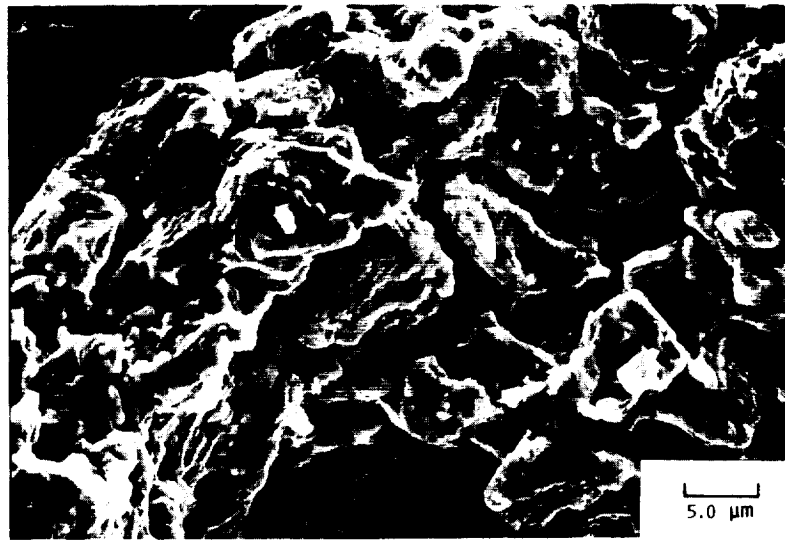
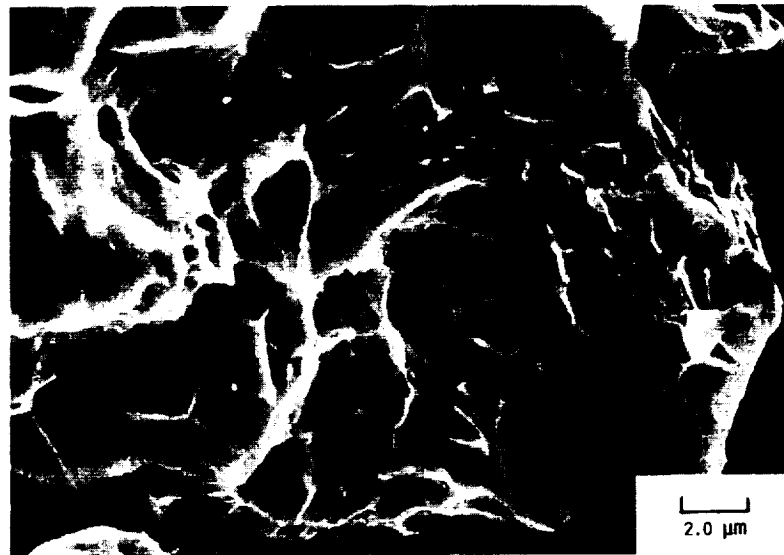


FIGURE 8. - SEM MICROGRAPH (BACK SCATTERED MODE) OF THE FATIGUE FRACTURE SURFACE OF A SPECIMEN TESTED AT 533 K WITH A MAXIMUM STRESS OF 240 MPa. BOTH MATRIX AND FIBER SHOW A DUCTILE FAILURE.

ORIGINAL PAGE
BLACK AND WHITE PHOTOGRAPH



(a) INTERGRANULAR FAILURE REGION.



(b) TRANSGRANULAR, DUCTILE OVERLOAD FAILURE REGION.

FIGURE 9. - MAGNIFIED SEM FRACTOGRAPHS OF THE Cu MATRIX FAILED AT 533 K.

ORIGINAL PAGE
BLACK AND WHITE PHOTOGRAPH

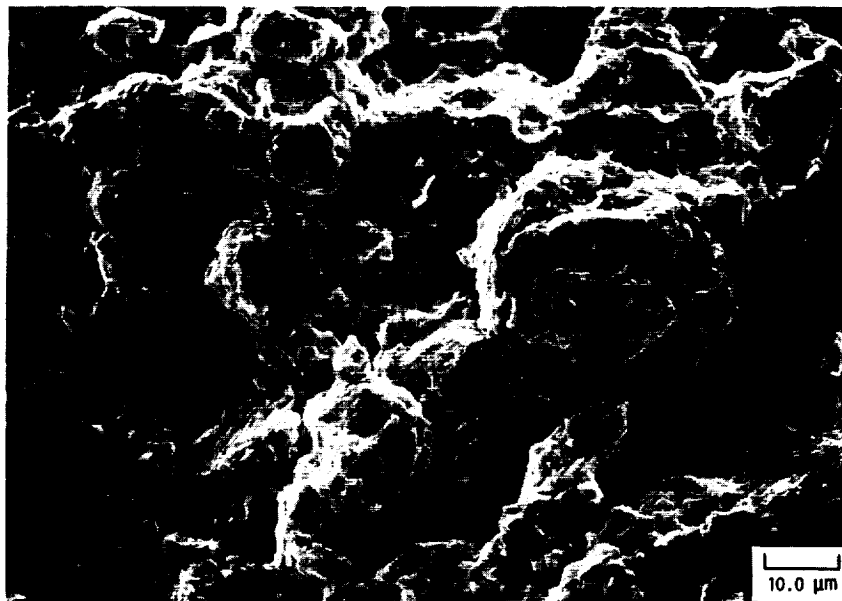


FIGURE 10. - SEM MICROGRAPHS OF A FATIGUE FRACTURE SURFACE FOR A SPECIMEN TESTED AT 833 K SHOWING AN INCREASED INTERGRANULAR FAILURE MODE IN THE CU MATRIX.

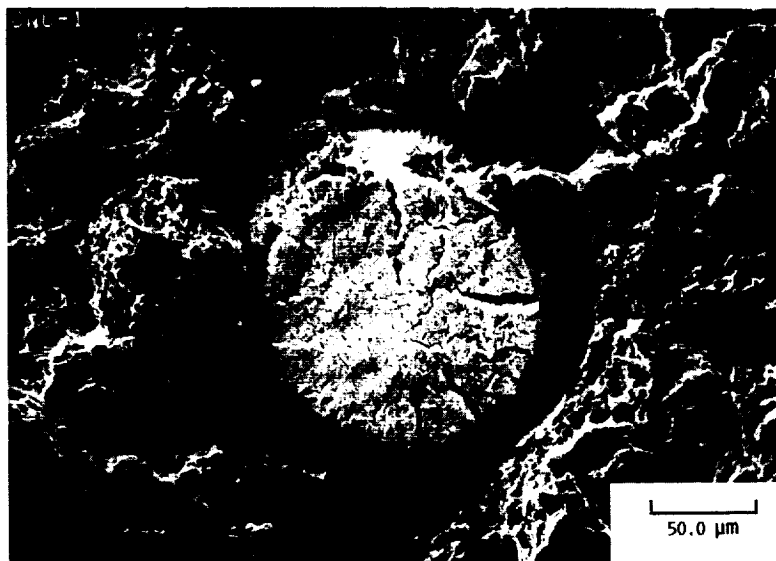


FIGURE 11. - SURFACE OF A CREEP-RUPTURE SPECIMEN TESTED UNDER A STATIC LOAD OF 240 MPa AT 533 K IN VACUUM. A PREDOMINANT INTERGRANULAR FAILURE MODE IS OBSERVED IN THE MATRIX.

ORIGINAL PAGE
BLACK AND WHITE PHOTOGRAPH

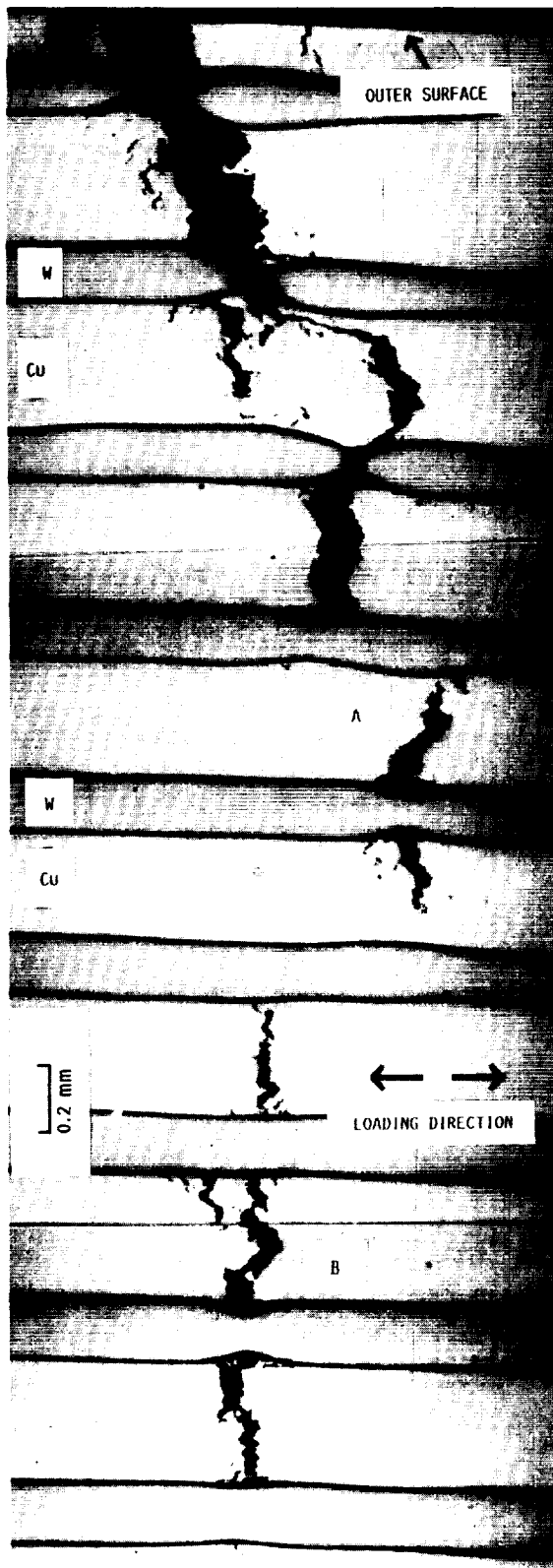


FIGURE 12. - LONGITUDINAL SECTION OF A FATIGUE SPECIMEN FRACTURED AT 533 K; MAXIMUM STRESS, 260 MPa; MINIMUM LOAD/MAXIMUM LOAD (R RATIO), 0.04. A, CRACK PROPAGATING FROM SPECIMEN SURFACE TO INTERIOR; B, INTERNALLY ORIGINATING CRACK.

ORIGINAL PAGE
BLACK AND WHITE PHOTOGRAPH

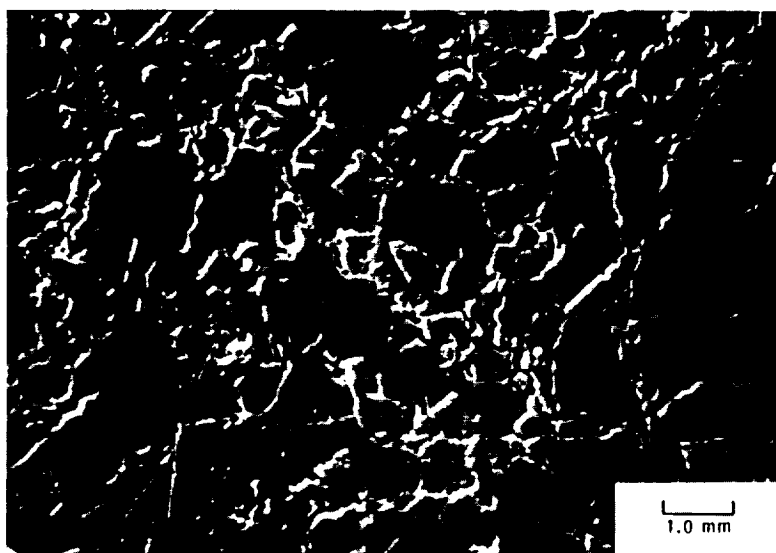


FIGURE 13. - SEM MICROGRAPH OF THE CU MATRIX OF A FATIGUE SPECIMEN FRACTURED AT 533 K. MANY GRAIN BOUNDARY, CAVITIES ARE REVEALED, AND SOME OF THEM ARE LINKED TO FORM MICROCRACKS.

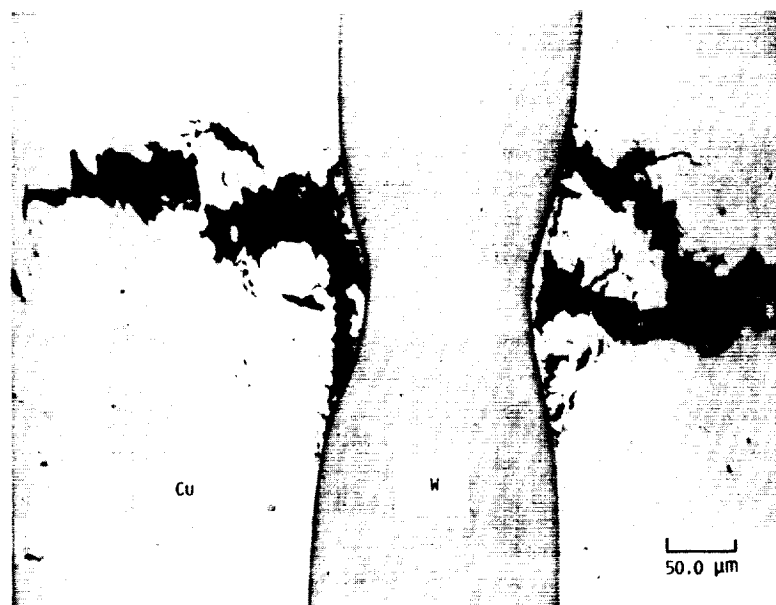
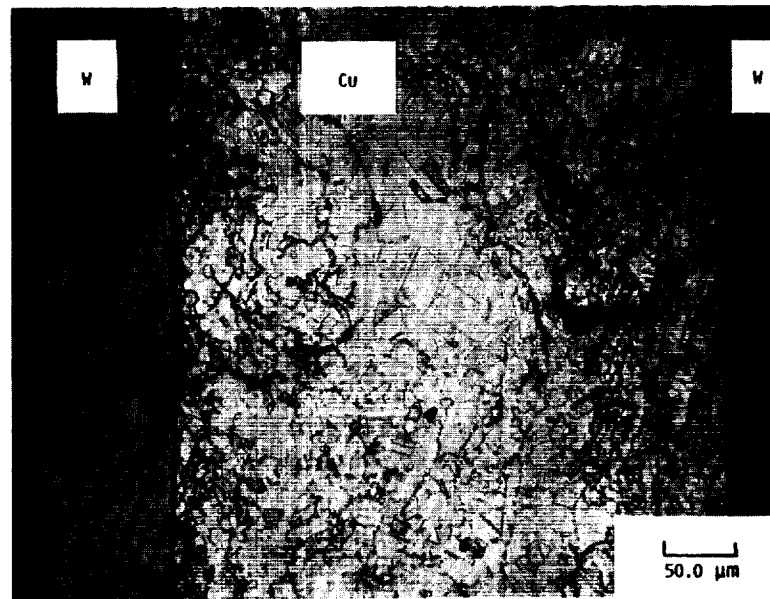


FIGURE 14. - OPTICAL MICROGRAPH SHOWING NECKING OF A TUNGSTEN FIBER AFTER FATIGUE AT 533 K.

ORIGINAL PAGE
BLACK AND WHITE PHOTOGRAPH



(a) CRACKS INITIATE AT FINE-GRAINED REGION.



(b) CRACKS PROPAGATE THROUGH FINE-GRAINED REGION.

FIGURE 15. - LONGITUDINAL SECTION OF A SPECIMEN FATIGUE FRACTURED AT 533 K SHOWING THE EFFECT OF GRAIN SIZE ON CRACK INITIATION AND PROPAGATION.

ORIGINAL PAGE
BLACK AND WHITE PHOTOGRAPH

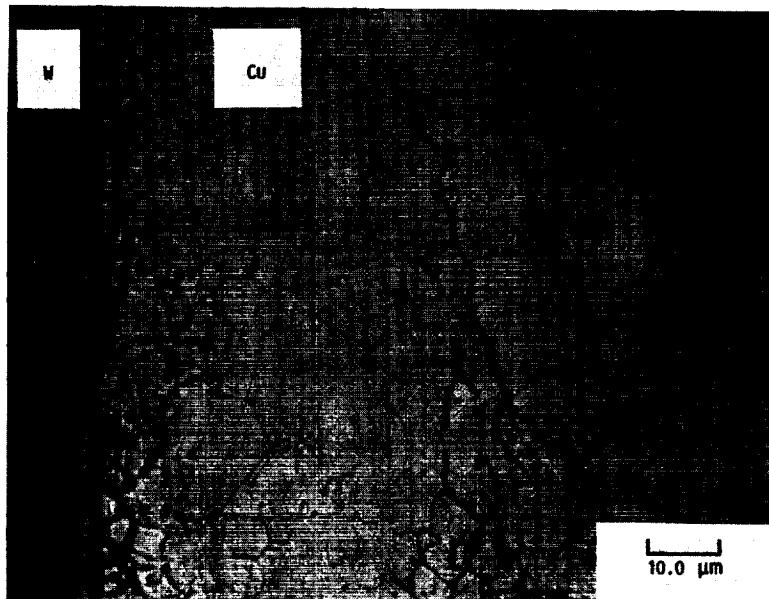


FIGURE 16. - LONGITUDINAL SECTION OF A FATIGUE SPECIMEN FRACTURED AT 533 K SHOWING UNEVEN DISTRIBUTION OF CAVITIES.



National Aeronautics and
Space Administration

Report Documentation Page

1. Report No. NASA TM-102371		2. Government Accession No.		3. Recipient's Catalog No.	
4. Title and Subtitle Characterization of Failure Processes in Tungsten Copper Composites Under Fatigue Loading Conditions				5. Report Date	
				6. Performing Organization Code	
7. Author(s) Yong-Suk Kim, Michael J. Verrilli, and Timothy P. Gabb				8. Performing Organization Report No. E-5090	
				10. Work Unit No. 553-13-00	
9. Performing Organization Name and Address National Aeronautics and Space Administration Lewis Research Center Cleveland, Ohio 44135-3191				11. Contract or Grant No.	
				13. Type of Report and Period Covered Technical Memorandum	
12. Sponsoring Agency Name and Address National Aeronautics and Space Administration Washington, D.C. 20546-0001				14. Sponsoring Agency Code	
15. Supplementary Notes Prepared for the International Symposium for Testing and Failure Analysis (ISTFA '89) sponsored by ASM International, Los Angeles, California, November 6-10, 1989. Yong-Suk Kim, National Research Council—NASA Research Associate.					
16. Abstract A fractographic and metallographic investigation was performed on specimens of a tungsten-fiber-reinforced copper matrix composite (9 vol%), which had experienced fatigue failures at elevated temperatures. The aim of the study was to determine major failure modes and possible failure mechanisms, with an emphasis placed on characterizing fatigue damage accumulation. Metallography of specimens fatigued under isothermal cyclic loading suggested that fatigue damage initiates in the matrix. Cracks nucleated within the copper matrix at grain boundaries, and they propagated through cavity coalescence. The growing cracks subsequently interacted with the reinforcing tungsten fibers, producing a localized ductile fiber failure. Examinations of interrupted tests before final failure confirmed the suggested fatigue damage processes.					
17. Key Words (Suggested by Author(s)) Fatigue (metal) Metal matrix composite Failure analysis			18. Distribution Statement Unclassified—Unlimited Subject Category 24		
19. Security Classif. (of this report) Unclassified		20. Security Classif. (of this page) Unclassified		21. No of pages 22	
				22. Price* A03	